Supplemental Figure 1.

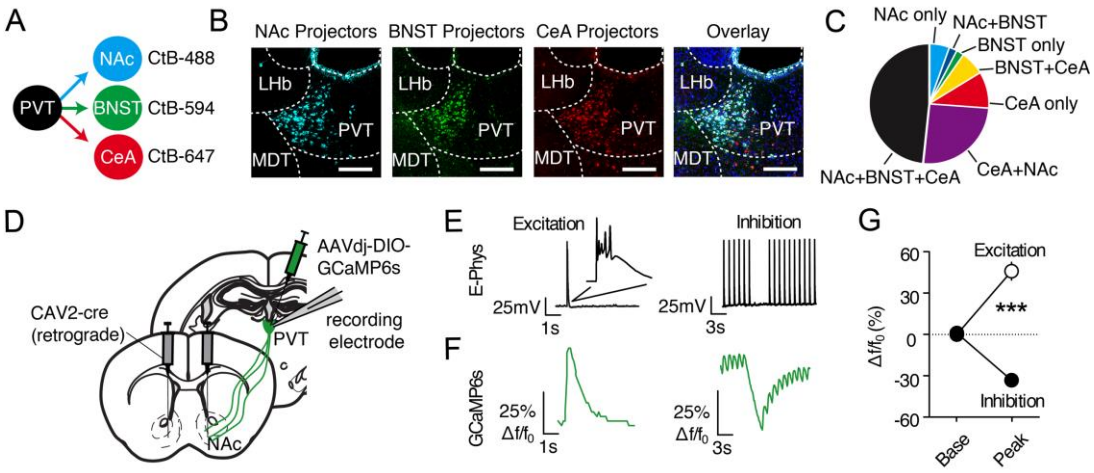

Supplemental Figure 1.

Associated with Figure 1: PVT projection neurons have bifurcating axons across the extended amygdala, and activity in these neurons can be tracked through the calcium indicator GCaMP6s.

(A) Retrograde tracers CtB-488, CtB-594, or CtB-647 were injected (n = 3 mice) unilaterally into the NAc, bed nucleus of the stria terminalis (BNST), and central amygdala (CeA).

(B) Confocal images showing that CtB injections resulted in retrograde labeling of PVT neurons that project to the NAc, BNST, and CeA. Scale bars represent 500 µm.

(C) Quantification of NAc-projecting, BNST-projecting, and CeA projecting neurons. Overall, 85% of labeled PVT neurons co-expressed 2 or 3 fluorophores, revealing that most of these PVT neurons project to more than one region of the extended amygdala.

(D) Viral strategy allowed patch-clamp recordings of GCaMP6s-expressing PVT-NAc neurons *ex vivo*.

(E) Example electrophysiological traces wherein action potentials were evoked through a single current pulse (Excitation, n = 7 cells), or wherein the same pulse was used to induce tonic firing (1 Hz) prior to a 3-second pause (Inhibition, n = 6 cells). All recorded PVT-NAc neurons were burst firing (see inset of 'Excitation'), such that each neuron either did not show spiking in response to current-induced depolarization, or showed multiple spikes before returning to threshold.

(F-G) Example fluorescent traces (F) and grouped data (G) visualized during electrophysiological recordings reveal that increases in action potential frequency provoked more fluorescence, whereas reductions in action potential frequency provoked less fluorescence (2-way ANOVA: $F_{1,11} = 104.0$, $p < 0.001$; *** indicates post-hoc $p < 0.001$). Data represent mean ± standard error.

Supplemental Figure 2

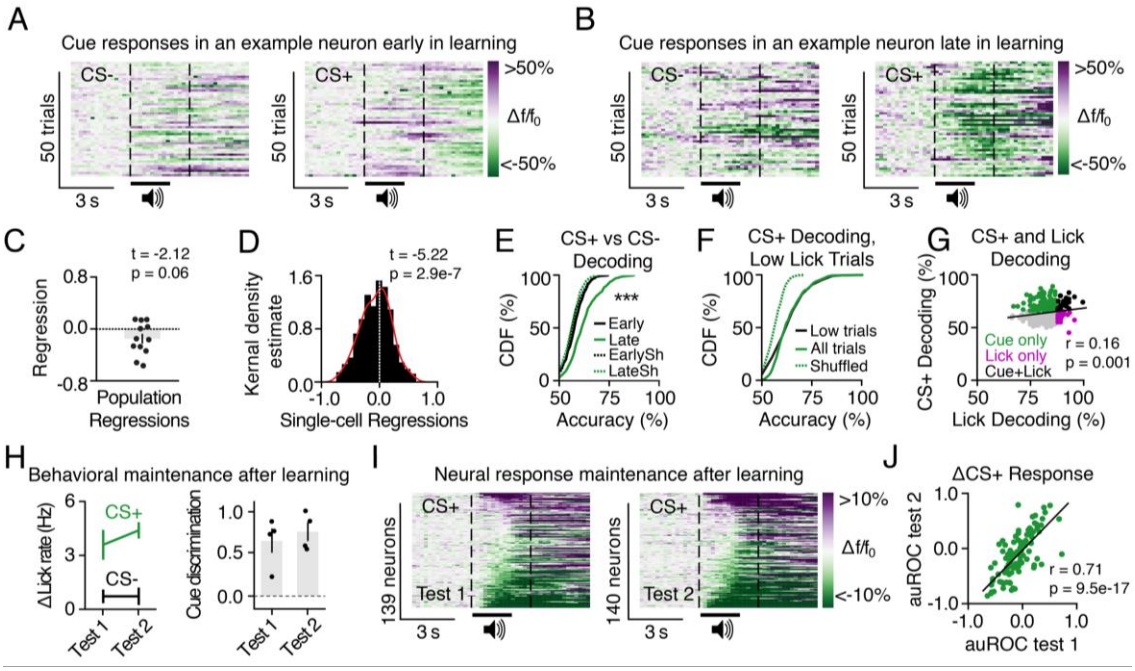

Supplemental Figure 2.

Associated with Figure 1: Cue responses in single PVT-NAc neurons are related to the cue-reward association and licking frequency.

(A-B) Heat plots from an example neuron early in learning (A) and late in learning (B) revealing single-trial CS- (left) and CS+ (right) calcium responses to reward-predictive cues.

(C) Regression values showing a trending negative relationship between licking and population response dynamics in PVT-NAc neurons in sessions late in learning (n = 7 mice, 12 sessions, 417 neurons averaged in each FOV; one-sample t-test: t_{11} = -2.12, p = 0.06). Data represent mean ± standard error.

(D) Histogram showing regression values for every recorded PVT-NAc neuron late in learning (n = 417), confirming a negative relationship between licking and single PVT-NAc neuronal responses (one-sample t-test: t_{416} = -5.22, $p < 0.001$).

(E) Cumulative distribution frequency (CDF) plots showing that the dynamics of individual PVT-NAc neurons could be used to predict whether the CS+ or CS- were presented late in learning (left, versus predictions early in learning: Welch's $t_{725.9}$ = 10.3, $p < 0.001$)

(F) Cumulative distribution frequency (CDF) plots showing that the dynamics of individual PVT-NAc neurons could be used to predict the timing of CS+ presentation during all trials ('All trials'; Welch's $t_{693.6}$ = 16.4, $p < 0.001$) and during trials wherein low licking rates are observed (i.e., the 10 lowest lick rate CS+ trials for each session; 'Low trials'; Welch's $t_{625.7}$ = 17.0, $p < 0.001$).

(G) Plotted CS+ and lick decoding responses in each recorded PVT-NAc neuron (n = 417), revealing a relationship between licking frequency decoding and CS+ association decoding (r = 0.16, p = 0.001). Despite this relationship, there were significant lick-only decoding cells (n = 45; pink circles), cue-only decoding cells (n = 137; green circles), and cells that decoded both (n =

25; black circles). Significant cue, lick, and cue+lick decoding cells were defined as those found to be 2 or more standard deviations above the respective shuffled mean.
(H) Grouped data showing that mice licked more during the CS+ versus CS- on two different sessions on separate days late in learning (left), resulting in consistent cue discrimination scores (right; n = 2 mice, 4 FOVs; independent t-test: $t_6 = 0.6$, $p = 0.57$). Data represent mean ± standard error.
(I) Population heat plots from PVT-NAc neurons showing averaged cue responses during the first session late in learning (left, n = 139 neurons) and during the second session late in learning (right, n = 140 neurons).
(J) Neuronal CS+ responses from all PVT-NAc cells tracked across the two sessions (n = 100 cells), showing that responses remained relatively stable for each particular neuron (Pearson correlation: $r = 0.71$, $p < 0.001$).

Supplemental Figure 3

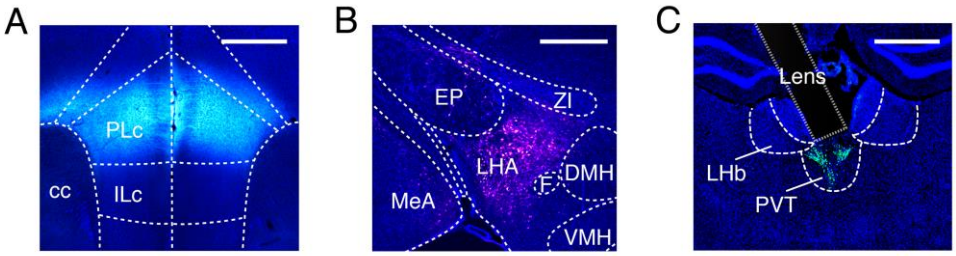

Supplemental Figure 3.
Associated with Figures 1-4: Histological verification of virus expression in PFC (A), LHA (B), and PVT (C). cc, corpus callosum; DMH; dorsomedial hypothalamus; EP, entopeduncular nucleus; F, fornix; ILc, infralimbic cortex; LHA, lateral hypothalamic area; LHb, lateral habenula; MeA, medial amygdala; PLc, prelimbic cortex; PVT, paraventricular thalamus; VMH, ventromedial hypothalamus; ZI, zona incerta. Scale bars represent 500µm.

Supplemental Figure 4

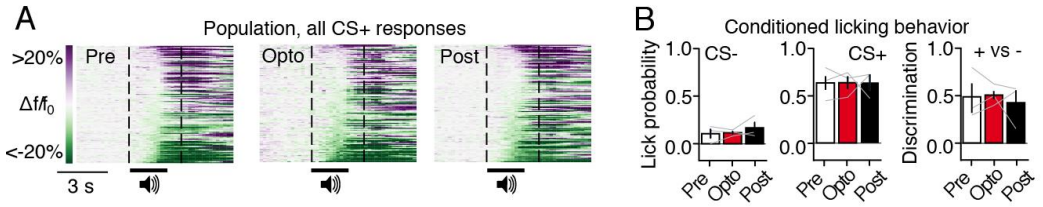

Supplemental Figure 4.
Associated with Figure 4. Activation of PFC inputs during the inter-trial-interval has no effect on PVT-NAc cue responses or behavioral cue discrimination.
(A) Population heat plot from all PVT-NAc neurons showing averaged CS+ responses during the Pre-Opto session (n = 2 mice, 3 FOVs, 115 neurons), during the Opto session (n = 2 mice, 3 FOVs, 116 neurons), and during the Post-Opto session (n = 2 mice, 3 FOVs, 119 neurons).
(B) Grouped behavioral data revealing equivalent lick probability during the CS- (left, repeated-measures ANOVA: $F_{2,4} = 0.9$, $p = 0.5$) and CS+ (middle, repeated-measures ANOVA: $F_{2,4} < 0.1$, $p = 1.0$), resulting in equivalent cue discrimination scores across sessions (right, repeated-measures ANOVA: $F_{2,4} = 0.2$, $p = 0.8$). Data represent mean ± standard error.